Journal of Power Technologies 101 (1) (2021) 78–85

Posted on Authorea 24 Mar 2021 — The copyright holder is the author/funder. All rights reserved. No reuse without permission. — https://doi.org/10.22541/au.161659439.90762749/v1 — This a preprint and has not been peer reviewed. Data may be preliminary.

Performance Enhancement of Shunt Active Power Filter Application using Adaptive Neural Network

Annu Govind[1,✉], Anupama Prakash[1], and Prakash Kumar[1]

[1]Amity University Uttar Pradesh
✉annugovind@gmail.com

Abstract

Adaptive neural network (ANN) topology-based control is proposed in this paper for three phase three wire shunt active power filter (SAPF) application. The proposed controller improves power quality and compensates harmonic components. The system includes a current controlled voltage source inverter (CC-VSI) using three phase insulated gate bipolar transistors (IGBT), a DSP module for generating regulated pulse width modulated (PWM) pulse and reference DC bus. The increase in nonlinear load applications has raised power quality issues. SAPF has emerged as one of the best solutions to improve power quality. Application of ANN in SAPF eliminates the need for unit template generation and the tuning requirement of phase locked loop (PLL), as required in traditional SAPF. The proposed ANN based SAPF can be dynamically regulated for minimum harmonic contamination. The results were obtained and verified in Matlab/ Simulink platform.

Keyword: DSP controller; harmonic minimization; neural network; power quality; shunt active power filter

1 Introduction

In recent decades power quality issues have been raised due to the increasing application of power electronic controllers, which include AC/DC/AC conversion and digital computational equipments used in interconnected electrical power networks [1, 2, 3]. These applications have nonlinear characteristics and cause harmonic pollution in power transmission/ distribution networks [4, 5].

The power-electronics converter & nonlinear loads are the main source of harmonics & reactive power, affectng power system performance [6, 7, 8, 9]. Voltage harmonics and related power distribution problems arise due to the current harmonics produced by nonlinear loads such as controlled/uncontrolled converter, electronic power supplies, lighting ballasts, arc furnaces, adjustable speed drives, electric oven and uninterruptible power supplies (UPS) [10, 11, 12]. Distorted voltage due to harmonics affects power quality for both power system operators and the consumers connected at the point of common coupling (PCC) [13, 14].

Passive and active filters are used extensively for improving the quality of power by overcoming current/voltage harmonics & compensating reactive power [15, 16, 17]. Usually, passive filtering has been preferred for harmonic compensation in the electrical power system due to its low cost, simplicity, reliability and efficient operation, but it has many disadvantages such as bulk, unsuitability for changing system conditions, source impedance strongly influencing the filtering characteristics and possibilities of anti-resonance with network impedance resulting in harmonic amplification [18, 19, 20, 21]. These drawbacks of passive filters and increasing power quality concerns need to be overcome by enhanced approaches towards mathematical analysis, robust design and ease of implementation of APFs [22, 23]. In series APFs voltage compensation signals are produced, whereas in shunts APFs current signal are obtained. APFs have better control and faster response than conventional passive filters. This paper deals with shunt APF control for minimization of the harmonic components involved.

2 System Configuration

The proposed shunt APF consists of a DSP control unit for processing voltage error signal and neural network logic for processing output parameters from the source. Fig. 1 shows the different components of the proposed system configuration for reactive power compensation and eliminating harmonics current components. The 3-phase power source was connected to a 3-phase uncontrolled converter having inductive-resistive *(RL)* / capacitive-resistive *(RC)* loads. The CC-VSI connected to a self-supported DC busbar (L_C, R_C) consists of standard self commutating IGBT switches. Series inductors (L_C, R_C) were

Posted on Authorea 24 Mar 2021 — The copyright holder is the author/funder. All rights reserved. No reuse without permission. — https://doi.org/10.22541/au.161659439.90762749/v1 — This a preprint and has not been peer reviewed. Data may be preliminary.

used to avoid high *di/dt* (Akagi et al., 2007).

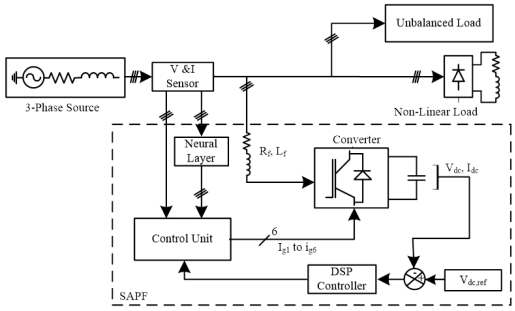

Figure 1: DSP-based three-phase SAPF

To eliminate switching spikes, three smoothing inductors (L_{sm}, R_{sm}) were coupled with a series nonlinear load. SAPF compensate the harmonic components & maintain the supply current sinusoidal by obtaining harmonic current of similar value and opposite phase.The capacitor connected on the dc side provides minor ripple in steady-state dc voltage. This capacitor stores energy and provides necessary real power during the transient period.

3 Control Strategy

The control technique used for reference current generation is simple, robust and has fast dynamic response under fixed and variable load conditions. It should also perform its best under non sinusoidal supply voltage condition. To attain it, the proposed control stratagem was divided into two steps. These two steps include estimation of reference source current using instantaneous p-q theory and fundamental signal extraction using the ANN algorithm.

3.1 Instantaneous p-q Theory

Fig. 2 shows a basic block diagram using the p-q theory control algorithm. It was designed for calculation of the reference source current.

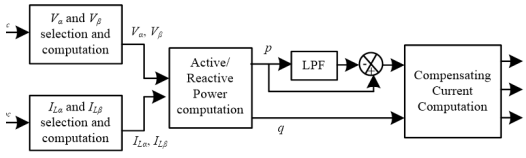

Figure 2: Schematic representation of reference current signal generation

s per p-q theory, instantaneous reactive power compensator encompassing devices like switching devices – which are passive components and do not need energy storage units. It can be used for compensation of a fundamental imaginary power component from harmonic current involved in instantaneous reactive load power under both steady state and transient conditions. Clarke Transformation was used for p-q theory. 3-phase voltage source voltage (v_{sa} , v_{sb} , v_{sc}) and load currents (i_{La} , i_{Lb} , i_{Lc}) were changed into an α-β-0 reference frame and calculated as [refer Equation (1)]

$$\begin{bmatrix} v_\alpha \\ v_\beta \\ v_0 \end{bmatrix} = [C] \begin{bmatrix} v_{sa} \\ v_{sb} \\ v_{sc} \end{bmatrix} and \begin{bmatrix} i_{L\alpha} \\ i_{L\beta} \\ i_{L0} \end{bmatrix} = [C] \begin{bmatrix} i_{La} \\ i_{Lb} \\ i_{Lc} \end{bmatrix}$$

$$where$$

$$[C] = \sqrt{2/3} \begin{bmatrix} 1 & -\frac{1}{2} & -\frac{1}{2} \\ 0 & \frac{\sqrt{3}}{2} & -\frac{\sqrt{3}}{2} \\ \frac{1}{\sqrt{2}} & \frac{1}{\sqrt{2}} & \frac{1}{\sqrt{2}} \end{bmatrix} \quad (1)$$

For balanced voltage condition, zero-sequence voltage is absent and current is available. In order to represent zero-sequence current and voltage components, *p* and *q* can be given as [refer Eq. (2)]

$$\begin{bmatrix} p \\ q \end{bmatrix} = \begin{bmatrix} v_\alpha v_\beta \\ -v_\beta v_\alpha \end{bmatrix} \begin{bmatrix} i_{L\alpha} \\ i_{L\beta} \end{bmatrix}$$
$$p = v_\alpha . i_{L\alpha} + v_\beta . i_{L\beta} \quad (2)$$
$$q = v_\alpha . i_{L\beta} - v_\beta . i_{L\alpha}$$

Thus, the instantaneous real and reactive power (q) can be calculated. Net power can be expressed as P_{net} represented as the sum of real and reactive power. This real and reactive power can further split in terms of DC (average) and AC (oscillating) components, given as [refer Eq. (3)]

$$p_{net} = p + q = \overline{p} + \tilde{p} + \overline{q} + \tilde{q} \quad (3)$$

Here, $\overline{p}$ and $\overline{q}$ and shows DC component of real and reactive power respectively. $\tilde{p}$ and $\tilde{q}$ are oscillating values of active and reactive power. These oscillations

Posted on Authorea 24 Mar 2021 — The copyright holder is the author/funder. All rights reserved. No reuse without permission. — https://doi.org/10.22541/au.161659439.90762749/v1 — This a preprint and has not been peer reviewed. Data may be preliminary.

of power occur between load and source without contributing to system energy. The α-β factors of load current are given as [refer Eq. (4)]

$$\begin{bmatrix} i_{L\alpha} \\ i_{L\beta} \end{bmatrix} = \frac{1}{v_\alpha^2 + v_\beta^2} \begin{bmatrix} v_\alpha - v_\beta \\ v_\beta v_\alpha \end{bmatrix} \begin{bmatrix} p \\ q \end{bmatrix} \tag{4}$$

Load current α-β component can be expressed on the basis of the average component and an instantaneous oscillating component of the real and imaginary power of the load.

$$i_{L\alpha} = \frac{v_\alpha}{v_\alpha^2 + v_\beta^2}.\bar{p} + \frac{v_\alpha}{v_\alpha^2 + v_\beta^2}.\tilde{p} + -\frac{v_\beta}{v_\alpha^2 + v_\beta^2}.\bar{q} + -\frac{v_\beta}{v_\alpha^2 + v_\beta^2}.\tilde{q}$$

$$i_{L\beta} = \frac{v_\beta}{v_\alpha^2 + v_\beta^2}.\bar{p} + \frac{v_\beta}{v_\alpha^2 + v_\beta^2}.\tilde{p} + -\frac{v_\alpha}{v_\alpha^2 + v_\beta^2}.\bar{q} + -\frac{v_\alpha}{v_\alpha^2 + v_\beta^2}.\tilde{q} \tag{5}$$

Equation (5) gives various components of load currents. To make the supply current smooth and distortion-free, currents should first flow from source to load; and compensate the other remaining reactive ($\bar{q}$) & oscillating ($\tilde{p}$, $\tilde{q}$) components; thereby improving overall power quality. Thus, the current control topology can be sub-divided into direct and indirect current control.

(a) In the d*irect current control (DCC) topology*, reference current (i^*_{ca} , i^*_{cb} , i^*_{cc}) is compared with filter current (i_{ca} , i_{cb} , i_{cc}).

(b) In i*ndirect current control (ICC)*, reference source current (i^*_{sa} , i^*_{sb} , i^*_{sc}) is compared with source current (i_{sa} , i_{sb} , i_{sc}).

These two current controlling techniques differ by their technique for reducing switching ripples. In the DCC topology, switching ripples are more as compared to ICC topology; as a reference, APF current operates on feed-forward control and varies rapidly compared to reference supply current, which operates on feedback control.

ICC topology has been used in this paper to generate a reference signal. To obtain average active power, α-β components are calculated from active power using load current and supply voltage. The zero/ dc power component is obtained from LPF with a tuned time constant. Now, the obtained V_{dc} and $V_{dc,ref}$ are compared and fed to the PI controller. The PI controller connected to the DC-link PCC compensates filter losses and regulates bus voltage. The PI controller output is processed error signal/loss power *(loss) [24, 25, 26]*. Therefore, the net active power of source (p') is the sum of zero components of active load power ($\bar{p}$) and obtained error signal *(p_{loss}))[refer Eq. (6)-(8)]*

$$p' = \bar{p} + p_{loss} \tag{6}$$

$$i^*_{s\alpha} = \frac{v_\alpha}{v_\alpha^2 + v_\beta^2}.p' \tag{7}$$

$$i^*_{s\beta} = \frac{v_\beta}{v_\alpha^2 + v_\beta^2}.p' \tag{8}$$

Equation (9) gives two-phase to three-phase transformation, using this three-phase instantaneous reference supply currents (i^*_{sa} , i^*_{sb} , i^*_{sc}) are to be computed.

$$\begin{bmatrix} i^*_{sa} \\ i^*_{sb} \\ i^*_{sc} \end{bmatrix} = \sqrt{2/3} \begin{bmatrix} 10 \\ -\frac{1}{2}\frac{\sqrt{3}}{2} \\ -\frac{1}{2} - \frac{\sqrt{3}}{2} \end{bmatrix} \begin{bmatrix} i^*_{s\alpha} \\ i^*_{s\beta} \end{bmatrix} \tag{9}$$

A hysteresis control based PWM converter was used to generate the desired pulses to obtain the regulated output.

3.2 Adaptive Neural Network Architecture

ANN architecture was used to extract a fundamental component from SAPF by minimizing harmonic pollution. It can be assured by estimating the reference current correctly in ideal and real time load applications for a given source voltage. In the context of increasing dependency on nonlinear loads in common households as well as industrial applications, minimization of harmonic pollution has been a prime challenge. When distorted voltage at PCC involves harmonic contamination in the source current and is further affected by additional harmonic contamination due to load current, ANN has been found more suitable than p-q theory in these cases of imprecise voltage.

Posted on Authorea 24 Mar 2021 — The copyright holder is the author/funder. All rights reserved. No reuse without permission. — https://doi.org/10.22541/au.161659439.90762749/v1 — This a preprint and has not been peer reviewed. Data may be preliminary.

This paper deals with a DSP based ANN controller for extraction of fundamental signal using the ICC scheme shown in Fig. 3. Source voltages (v_{sa} , v_{sb} , v_{sc}) are first transformed into a two phase (v_α & v_β) component. An adaptive linear (ADALINE) network based ANN was established to obtain primary voltage components $v_{\alpha,\varphi}$ & $v_{\beta,\varphi}$ from distorted v_α & v_β components. Primary voltage components were used to calculate the active power transmitted from source to load in a 3-phase system. The ANN (ADALINE) used in this paper has two neural layers in feed forward control topology, having "n" inputs and single output. The output signal depends on training data and pattern; thereby providing a trained ANN block for generation of regulated source voltage.

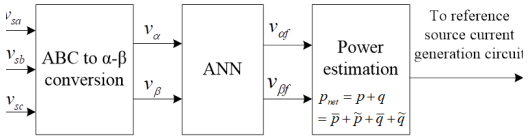

Figure 3: Reference Current Generation using ANN

Voltage input weight factors in the proposed ADALINE network was given as $V = (v_{1n}, v_{2n}, v_{3n},\ldots v_{mn})^T$ and $W = (w_{1n}, w_{2n}, w_{3n},\ldots w_{mn})^T$, respectively. Considering a linear transfer function with Y_0 bias, the obtained outcome Y in terms of voltage input and weight for nth function is calculated as [refer Eq.(10)]

$$Y_{(n)} = W^T_{(n)}.V_{(n)} = Y_0 + w_{1n}v_{1n} + w_{2n}v_{2n} + w_{3n}v_{3n} + .. = Y_0 + \quad (10)$$

Adaption of the weight was done by *Widrow-Hoff delta rule*, also termed as Least mean square (LMS) in the presented ADALINE network. It minimizes the mean square error between the expected and obtained output y (n). It can be represented as [refer Eq. (11)]

$$w_{(n+1)} = w_{(n)} + \alpha \frac{e_{(n)}v_{(n)}}{|v_{(n)}|^2} \quad (11)$$

Where, $w(n+1)$ and $w(n)$ represent the next and present value of weight vector respectively, $v(n)$ and $e(n)$ show the input (voltage) error signal. The value of α was calculated by the current decomposition technique.

4 Simulation and Results

The presented system and ANN were validated on the Matlab/ Simulink platform. The system under consideration is shown in Fig.4

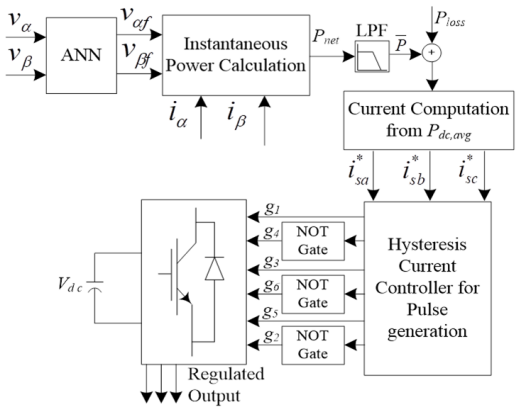

Figure 4: Proposed ANN architecture for APF

The factors of source voltage, APF and load have been simulated as listed in Table 1. Simulated results have been obtained to verify the working of proposed neural network for the APF with balanced and nonlinear load conditions. The three phase source voltage and current used in this paper has been shown in the Fig. 5 and Fig. 6 respectively.

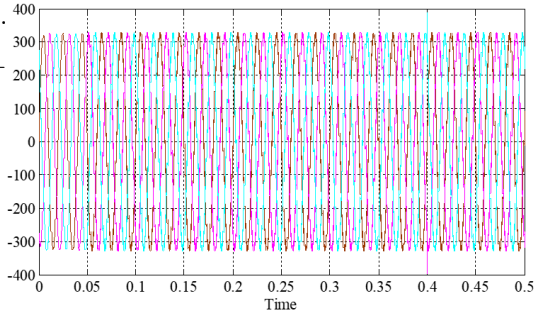

Figure 5: Voltage source output voltage in volts

The obtained THD is nominal for source voltage and current as 1.12% and 3.12% respectively, as shown in Fig. 7 and Fig. 8. Now a load of 7.5 kW has initially been connected to the source at 0.05 Sec. At this instant when APF is switched ON, the obtained source current is changed to sinusoidal as of stepped waveform. Thus, the obtained DC capacitor voltage achieves steady state voltage magnitude, in contrast to the reference voltage magnitude, in a few consec-

Posted on Authorea 24 Mar 2021 — The copyright holder is the author/funder. All rights reserved. No reuse without permission. — https://doi.org/10.22541/au.161659439.90762749/v1 — This a preprint and has not been peer reviewed. Data may be preliminary.

Table 1: The APF parameters used for simulation

System parameters	Simulated values
Supply voltage (Vs)	230 volts/ph, 50 Hz
Cdc, Vdc	1.5 * 102 µF, 612 volt
Coupling inductors (Rc, Lc)	0.2 Ω, 2.75 mH
Source impedance (Rs , Ls)	0.1 Ω , 0.25 mH
Smoothing inductor (Rsm, Lsm)	0.1 Ω, 1 mH
(RL1, LL1) and (RL2, LL2)	(50 Ω, 20 mH) , (100 Ω, 16 mH)

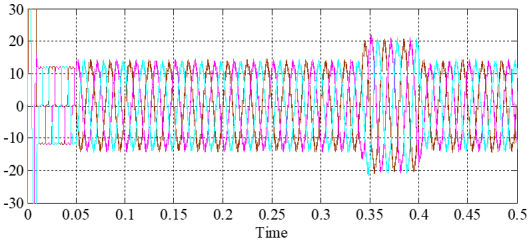

Figure 6: Voltage source output current in amps

utive cycles as obtained in Fig. 9. To analyze the system behavior for variable load condition, load has been changed from 7.5 kW to 10 kW at t=0.34 s by changing the balanced load and again changed from 10 kW to 7.5 kW at t=0.4 s.

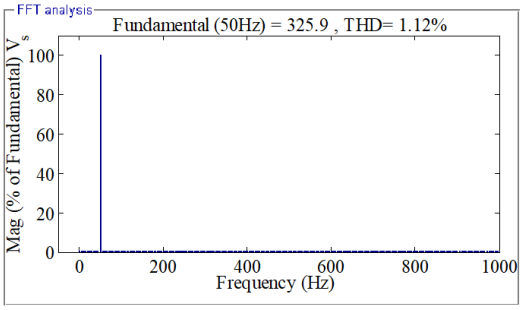

Figure 7: THD of voltage source output voltage

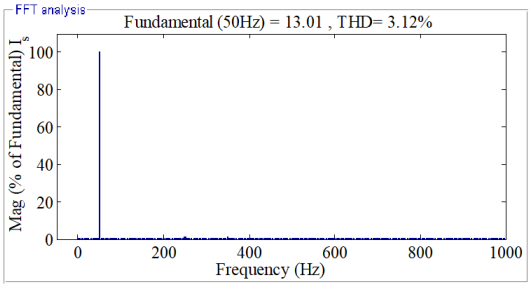

Figure 8: THD of voltage source output current

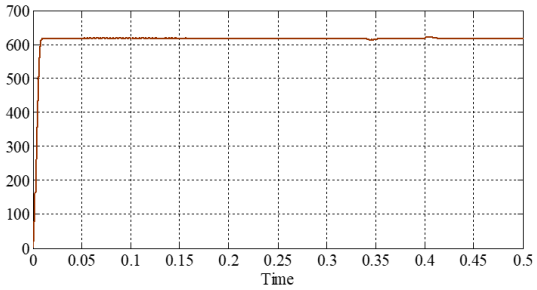

Figure 9: Voltage across the capacitor for balanced load

To check the robustness of the proposed system, distorted nonlinear current and voltage was considered, as shown in Fig. 10 and Fig. 11 respectively. The obtained V_{DC} is highly distorted and compensating current, as shown in Fig. 12, has been used.

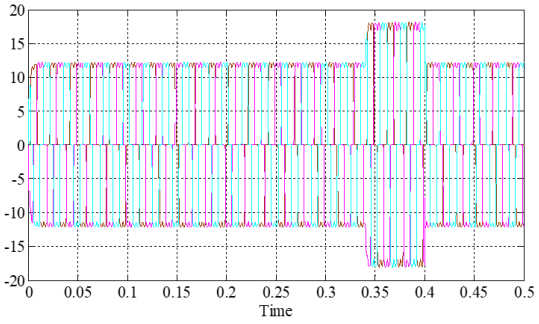

Figure 10: Nonlinear current due to nonlinear load

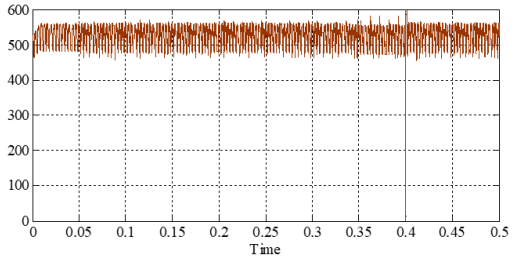

Figure 11: Distorted voltage due to nonlinear load

Posted on Authorea 24 Mar 2021 — The copyright holder is the author/funder. All rights reserved. No reuse without permission. — https://doi.org/10.22541/au.161659439.90762749/v1 — This a preprint and has not been peer reviewed. Data may be preliminary.

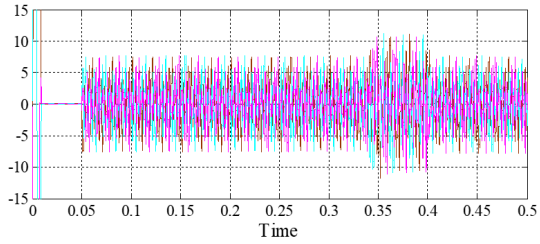

Figure 12: Compensating current

In order to reduce higher order harmonics, ANN was incorporated to generate reference voltage signal by extracting fundamental voltage component from distorted voltage waveform. This reference voltage signal is converted into alfa and beta components and then passed through a DSP unit to generate the required PWM signal for obtaining line fundamental voltage and current components as obtained in Fig. 13. The response of the trained neural network has been seen in less than one cycle time period. Obtained line voltage and current has been shown in Fig. 14. Thus obtained regulated PWM pulses can be used to obtain desired regulated volage and current at the output terminals. The obtained output has THD of 4.52%, as shown in Fig. 15.

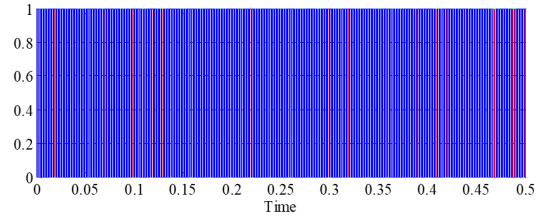

Figure 13: Generated PWM waveform from the ANN-DSP module

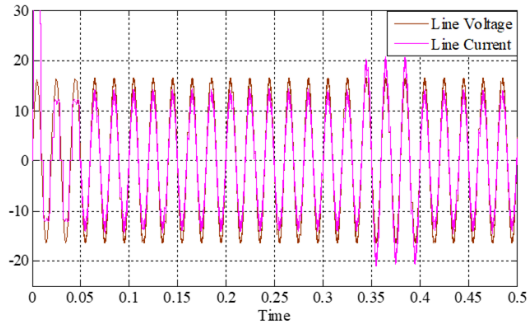

Figure 14: Obtained line voltage and current waveform

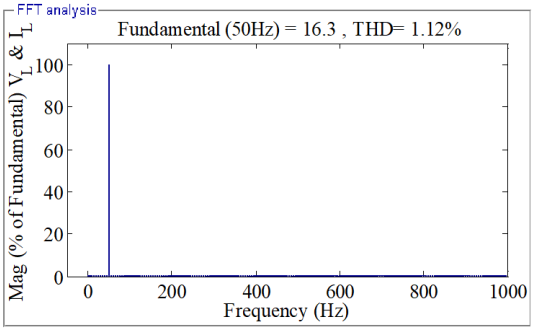

Figure 15: Obtained THD in output line voltage and current

5 CONCLUSION

A neural network-based controller is proposed in this paper for a three-phase three-wire shunt APF. To validate the compatibility of the proposed approach, an indirect current control theory-based controller was developed for variable loads at different switching instant. To generate the reference source current instantaneous p-q theory with indirect current control technique is used and the switching pattern of semiconductor devices used in the PWM converter. The performance of the proposed APF was evaluated in Matlab/ Simulink platform. The obtained THD is within the permissible limit of 10% for both uniform and nonlinear loading condition. Compared to the direct current control technique, the indirect current control technique is superior for eliminating switching ripples from the supply current. The obtained results reveal satisfactory operation of the system at hand, under sudden load and frequency changes conditions.

Acknowledgement

I would like to express my deep gratitude to Professor D.K.Palwalia for his valuable & enthusiastic encouragement for this research work. I would also like to thank Dr. V.K.Tayal and Dr. Prakash Kumar, my research supervisors, for their patient guidance and useful critiques for this research work. My thanks are also extended to Mr. Kuldeep Jayaswal for his valuable and constructive suggestions during the planning and development of this article.

Finally, I wish to thank my husband and my kids for their support and encouragement throughout my work.

Posted on Authorea 24 Mar 2021 — The copyright holder is the author/funder. All rights reserved. No reuse without permission. — https://doi.org/10.22541/au.161659439.90762749/v1 — This a preprint and has not been peer reviewed. Data may be preliminary.

References

[1] Nitin Gupta, S. P. Singh, S. P. Dubey, and D. K. Palwalia. Digital Signal Processor based Performance Investigation of Indirect Current Controlled Active Power Filter for Power Quality Improvement. *International Journal of Emerging Electric Power Systems*, 13(2), jun 2012.

[2] Tuopu Na, , Qianfan Zhang, Jiaqi Tang, Jinxin Wang, , and and. Active Power Filter for Single-Phase Quasi-Z-Source Integrated On-Board Charger. *CPSS Transactions on Power Electronics and Applications*, 3(3):197–201, sep 2018.

[3] Prakash Kumar, Dip Vinod Thanki, Maneet Kour, and Harnek Singh. Single Phase Five Level Inverter for Solar-PV Applications. In *2018 International Conference on Intelligent Circuits and Systems (ICICS)*. IEEE, apr 2018.

[4] Yigeng Huangfu, Shengzhao Pang, Babak Nahid-Mobarakeh, Liang Guo, Akshay Kumar Rathore, and Fei Gao. Stability Analysis and Active Stabilization of On-board DC Power Converter System with Input Filter. *IEEE Transactions on Industrial Electronics*, 65(1):790–799, jan 2018.

[5] D. K. Palwalia and S. P. Singh. Digital Signal Processor-based Controller Design and Implementation for Self-excited Induction Generator. *Electric Power Components and Systems*, 36(10):1130–1140, sep 2008.

[6] Zhiheng Lin and Xinbo Ruan. A Three-Phase Adaptive Active Damper for Improving the Stability of Grid-Connected Inverters Under Weak Grid. In *2019 IEEE Applied Power Electronics Conference and Exposition (APEC)*. IEEE, mar 2019.

[7] Prakash Kumar and D. K. Palwalia. Static Voltage and Frequency Regulation of Standalone Wind Energy Conversion System. *Indian Journal of Science and Technology*, 9(29), aug 2016.

[8] Harnek Singh, Maneet Kour, Dip Vinod Thanki, and Prakash Kumar. A Review on Shunt Active Power Filter Control Strategies. *International Journal of Engineering & Technology*, 7(4.5):121, sep 2018.

[9] K Jayaswal, DK Palwalia, and S Kumar. Analysis of robust control method for the flexible manipulator in reliable operation of medical robots during COVID-19 pandemic. *Microsyst Technol*, pages 1–14, Oct 2020.

[10] Junpeng Ji, Wenjie Chen, Xu Yang, and Jingjie Lu. Delay and Decoupling Analysis of a Digital Active EMI Filter Used in Arc Welding Inverter. *IEEE Transactions on Power Electronics*, 33(8):6710–6722, aug 2018.

[11] Prakash Kumar and Dheeraj Kumar Palwalia. Decentralized Autonomous Hybrid Renewable Power Generation. *Journal of Renewable Energy*, 2015:1–18, 2015.

[12] B. Singh, K. Al-Haddad, and A. Chandra. A review of active filters for power quality improvement. *IEEE Transactions on Industrial Electronics*, 46(5):960–971, 1999.

[13] Yong Wang, Jialong Xu, Ling Feng, and Chengmin Wang. A Novel Hybrid Modular Three-Level Shunt Active Power Filter. *IEEE Transactions on Power Electronics*, 33(9):7591–7600, sep 2018.

[14] D. K. Palwalia and S. P. Singh. Digital Signal Processor Based Fuzzy Voltage and Frequency Regulator for Self-excited Induction Generator. *Electric Power Components and Systems*, 38(3):309–324, jan 2010.

[15] D.K. Palwalia. DSP-based fuzzy load controller for single phase self-excited induction generator. *International Journal of Power Electronics*, 3(5):453, 2011.

[16] Seema Agrawal, Prakash Kumar, and D. K. Palwalia. Artificial neural network based three phase shunt active power filter. In *2016 IEEE 7th Power India International Conference (PIICON)*. IEEE, nov 2016.

[17] Prakash Kumar, Gaurav Jain, and Dheeraj Kumar Palwalia. Genetic algorithm based maximum power tracking in solar power generation. In *2015 International Conference on Power and Advanced Control Engineering (ICPACE)*. IEEE, aug 2015.

[18] Pulkit Singh Shantanu Kumar Sharma. Modeling and Simulation of Photovoltaic with Fuzzy and Power Management of Hybrid System. *International Journal of Advanced Research in Electrical, Electronics and Instrumentation Engineering*, 04(06):5143–5152, jun 2015.

[19] A. Chebabhi, K. Abdelhalim, Fellah Mohammed Karim Fellah, and Amrane Fayssal. Self Tuning Filter and Fuzzy logic Control of Shunt Active Power Filter for Eliminates the Current Harmonics Constraints under Unbalanced Source Voltages and Loads Conditions. *Journal of Power of Technologies*, 98:1–19, 2018.

[20] B. Subudhi, R. Panigrahi, and P. C. Panda. A Comparative Assessment of Hysteresis and Dead Beat Controllers for Performances of Three Phase Shunt Active Power Filtering. *Journal of Power of Technologies*, 94:286–295, 2014.

[21] Prakash kumar Dheeraj kumar palwalia Kuldeep jayaswal, Gaurav jain. Design-Oriented Analysis of Non-isolated DC-DC Buck Converter. *Ciência e Técnica Vitivinícola Journal, Portugal*, 30, 2015.

[22] Cheng Nie, Yue Wang, Wanjun Lei, Mingfeng Chen, and Yan Zhang. An Enhanced Control Strategy for Multiparalleled Grid-Connected Single-Phase Converters With Load Harmonic Current Compensation Capability. *IEEE Transactions on Industrial Electronics*, 65(7):5623–5633, jul 2018.

[23] Lei Wang, Chi-Seng Lam, and Man-Chung Wong. Analysis Control, and Design of a Hybrid Grid-Connected Inverter for Renewable Energy Generation With Power Quality Conditioning. *IEEE Transactions on Power Electronics*, 33(8):6755–6768, aug 2018.

[24] Mustapha Muhammad Saidu, Shiva Pujan Jaiswal, Kuldeep Jayaswal, Shibamay Mitra, and Vikas Singh Bhadoria. A survey on: Automation of micro grid and micro distributed generation. *Materials Today: Proceedings*, dec 2020.

[25] Kalpana Meena, Kuldeep Jayaswal, and D. K. Palwalia. Analysis of Dual Active Bridge Converter for Solid State Transformer Application using Single-Phase Shift Control Technique. In *2020 International Conference on Inventive Computation Technologies (ICICT)*. IEEE, feb 2020.

[26] K. Jayaswal and D. K. Palwalia. Performance Analysis of Non-Isolated DC-DC Buck Converter Using Resonant Approach. *Engineering, Technology & Applied Science Research*, 8(5):3350–3354, oct 2018.

Posted on Authorea 24 Mar 2021 — The copyright holder is the author/funder. All rights reserved. No reuse without permission. — https://doi.org/10.22541/au.161659439.90762749/v1 — This a preprint and has not been peer reviewed. Data may be preliminary.